# International Journal of Heat and Technology

Vol. 43, No. 1, February, 2025, pp. 335-344

Journal homepage: http://iieta.org/journals/ijht

# Numerical Investigation of Axisymmetric Jet Impingement Heat Transfer on a Flat Plate **Equipped with Vortex Generator**



Mohamed Nedjmeddine Belaib\* Adra Benhacine, Rahima Benchabi

LEAP, Mechanical's Engineering Department, University of Mentouri Brothers Constantine 1, Constantine 25000, Algeria

Corresponding Author Email: mohamednedjmelddine.belaib@doc.umc.edu.dz

Copyright: ©2025 The authors. This article is published by IIETA and is licensed under the CC BY 4.0 license (http://creativecommons.org/licenses/by/4.0/).

https://doi.org/10.18280/ijht.430134

Received: 21 December 2024 Revised: 2 February 2025 Accepted: 16 February 2025 Available online: 28 February 2025

Keywords:

CFD study, impinging axisymmetric jet, heat transfer, Nusselt number, SST k-ω model, vortex generators

#### **ABSTRACT**

This study investigates heat transfer enhancement between a turbulent air jet and a flat wall using an axisymmetric vortex generator in the form of a tab. The number of Reynolds ranged 10,000 to 50,000, and the spacing between the jet nozzle and the impingement surface ranged from 0.5 D to 6 D. The vortex generator influence on heat transfer was simulated by adjusting its height e  $(0.5 < e/\delta < 2)$  and location L (0.25 < L/D < 2). The SST k-ω model was used, validated against relevant experimental data. The local heat transfer distributions on the target surface were studied, with a particular focus on the vortex generator region. The findings indicated the presence of a recirculation zone behind the tab, which is responsible for enhancing heat transfer. when the tab is set at a height matching the boundary layer thickness and positioned at 0.7 D from the axis, the maximum improvement in PEC and the average Nusselt number Nu is achieved, reaching 3.8%. Additionally, Correlations were proposed for calculating average Nu based on the Re and geometric parameters (H, e and L).

# 1. INTRODUCTION

Jet impingement technology offers a potent method for boosting transfer efficiency. many industrial processes utilize this technique, including drying papers, food products, textiles, processing certain metals and glass, it is also employed in cooling gas turbine blades, combustion chamber walls, and electronic equipment. Numerous parameters affect heat transfer rates, including the Re, H/D, Roughness, inclination, curvature of the target plate, Prandtl number, nozzle geometry and turbulence intensity at the entrance of the jet. Among the studies conducted on a jet impingement with a flat surface were reported [1-3] several parameters were investigated aimed at enhancing heat transfer. Nakod et al. [4] conducted experimental research to investigate the effect of surfaces equipped with vortex generators and surfaces with fins. The Re number ranged from 7,000 and 30,000. H/D, Re, number and radius of rows, as well as the angle of inclination of VGs were examined. the results demonstrated the effectiveness of the surface equipped with a single row of six VGs in providing the best heat transfer. Ortega-Casanova and Molina-Gonzalez [5] researchers numerically simulated turbulent flow of an axisymmetric jets impinging on flat walls equipped with vortex generators. The Re, H/D, the height of the ribs, and their position were examined. The results indicated that recirculation zones downstream the tab and the vorticity at the tip of the tab are responsible for improving the Nusselt number. Takeishi et al. [6] conducted experimental investigations on heat transfer from jet impingement on flat plates fitted with circular ribs or vortex generators. Different heights and positions of the vortex generators were tested, and it was found

that adjusting the height of the vortex generator to match the boundary layer thickness results in optimal heat transfer. The results also revealed an augment in  $\overline{Nu}$  by up to 51% for vortex generators and up to 21% for circular ribs within the tested geometries. The same result was obtained by Alenezi et al. [7]. In their numerical analysis, the roughness element achieved a 15.6% enhancement in the average Nusselt number when the rib height was set near the boundary layer thickness. They also found that inserting the rib in the stagnation zone was ineffective for heat transfer enhancement. A study was conducted on the effect of convective heat transfer resulting from the impact of airflow on a ribbed surface. Three types of rib configurations were investigated, and the effect of jet-totarget distance was tested at different Reynolds numbers (6,000-30,000). The ribs enhanced convective heat transfer by up to 30% compared to a smooth surface. Inverted V-shaped ribs demonstrated the highest efficiency in improving heat transfer, especially at short jet-to-target distances [8]. Kotb et al. [9] conducted to investigate the effect of vortex air jets on enhancing heat transfer. A new vortex generator of the blade type was used to produce vortex flow. The experimental analysis focused on comparing traditional air jets with vortex jets at different vortex numbers and nozzle-to-plate distances. Zeiny et al. [10] numerical simulations were performed on an impinging plate equipped with obstacles, using a twisted ribbon in the nozzle to induce vortex flow. The results showed a 29% increase in  $\overline{Nu}$  with a single obstacle, an H/D=2, and a twisted tape with 12 turns. The average Nu number increases directly with the increase in the twists number. The research focused on a specific work of studies [11, 12] where it was found that delta winglet pairs generated noticeable longitudinal vortex pairs in the downs weep zone, leading to enhanced heat transfer. Results showed that delta-winglet generators outperformed rectangular winglets in terms of heat transfer improvement. Ali et al. [13] presented for the development of solid vortex generator shapes. The optimal design achieved a thermal performance factor of 1.28, with a 6% enhancement in heat transfer and only a 13% increase in pressure drop. Bansode et al. [14] presented an innovative VG design with slotted fins was proposed, which proved effective in enhancing the thermohydraulic performance of heat exchangers. Another work of Caliskan [15], a novel model for perforated triangular and rectangular VGs was developed, achieving a 50% improvement in heat transfer for punched triangular VG. Tian et al. [16] conducted a computational investigation to examine the effect of rectangular and deltawinglet VGs on heat transfer. The results showed the efficiency of rectangular VGs in heat transfer, achieving an increase of approximately 45%. Oda and Takeishi [17] presented an analysis to examine the influence of square and circular ribs on heat transfer, employing Large Eddy Simulation. They observed enhanced heat transfer following flow reattachment behind the ribs and validated their findings by comparing RANS and LES with experimental data. The study concluded that LES effectively captured the majority of experimental phenomena, with the turbulent shear layer formed behind the rib boosting turbulent heat transfer around the reattachment region, notably, that the optimal value of the heat transfer coefficient occurs when the rib height matches the boundary layer thickness  $\delta$ . Further LES investigations were conducted in works of Dutta et al. [18, 19] regarding heat transfer from slot jet impingement. They discovered that LES effectively captures the majority of experimental phenomena, with predictions closely aligning with reported experimental results. Shukla and Dewan [20] conducted a computational study using various turbulence models to evaluate their suitability for jet impingement on both flat and ribbed surfaces. The objective was to anticipate flow and heat transfer properties across different Re numbers and jet-plate distance H/D. The results revealed that the SST k-ω model demonstrated excellent performance for low H/D, while the standard k-ε model excelled for elevated H/D. Moreover, an increase in rib pitch was associated with a rise in the Nu close the stagnation zone, followed by a decrease downstream.

Based on the reviewed studies mentioned in the literature [5-7], transverse vortex generators are believed to show positive results in enhancing heat transfer. However, there has been limited research on modifying the height and position of the ribs.

The present work presents a numerical study on the thermal effects of a turbulent axisymmetric jet impinging on a surface equipped with a small tab. A detailed parametric analysis was conducted to explore the effects of the Reynolds number, nozzle-to-plate spacing, vortex generator height and position, and PEC analysis to determine the optimal configurations to enhance heat transfer efficiency, Flow and heat transfer characteristics were also evaluated using different turbulence models for both the flat and tabbed plates and compared with experimental results. Notably, the study establishes correlations for both the average Nusselt number and the stagnation Nusselt number, providing a quantitative framework for understanding their dependence on critical factors. The analysis focuses on the Re number ranging from 10,000 to 50,000, along with geometric parameters within specified limits  $(0.5 < H/D < 6, 0.25 < L/D < 2, and 0.5 < e/\delta)$ 

< 2). These results not only provide practical guidelines for improving heat transfer but also contribute to a deeper understanding of the underlying fluid dynamics.

#### 2. MATHEMATICAL FORMULATION

#### 2.1 Problem description

Figure 1 depicts the numerical domain investigated in this study, which is an axisymmetric jet with a diameter D=4 mm. The distance H between the jet nozzle and the impingement surface ranged from 0.5 to 6 times the nozzle diameter. The impingement plate radius is R=6 D, and the normalized tab height  $e/\delta$  varies from 0.5 to 2. Additionally, the tab location L/D, measured from the stagnation point, is changed between 0.25 and 2. The Re is ranges from 10,000 to 30,000.

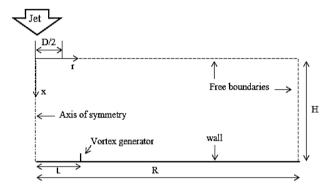


Figure 1. Numerical domain with boundary conditions

### 2.2 Governing equations

In this work the fluid considered is the air which is Newtonian and incompressible. The flow is steady, axisymmetric and turbulent. It is governed by the Eqs. (1), (2) and (3) in compact notation which represent the continuity, momentum and energy equations respectively.

$$\frac{\partial V_i}{\partial x_i} = 0 \tag{1}$$

$$\frac{\partial (V_i V_j)}{\partial x_i} = -\frac{1}{\rho} \left[ \frac{\partial P}{\partial x_i} \right] + \frac{\mu}{\rho} \frac{\partial}{\partial x_j} \left[ \frac{\partial V_i}{\partial x_j} + \frac{\partial V_j}{\partial x_i} \right] + \frac{\partial (-\overline{u_i u_j})}{\partial x_j} \tag{2}$$

$$\frac{\partial (V_j T)}{\partial x_j} = \frac{\partial}{\partial x_j} \left[ \alpha \frac{\partial T}{\partial x_j} \right] + \frac{\partial (-\overline{u_j t})}{\partial x_j}$$
 (3)

where,  $-\overline{u_i u_j}$  denotes the Reynolds stress tensor. Based on the Boussinesq concept, it is expressed as following Eq. (4).

$$-\overline{\mathbf{u}_{i}}\overline{\mathbf{u}_{j}} = \frac{\mu_{t}}{\rho} \left[ \frac{\partial V_{i}}{\partial x_{i}} + \frac{\partial V_{j}}{\partial x_{i}} \right] - \frac{2}{3} \mathbf{k} \delta_{ij}$$
 (4)

and  $\overline{u_i t}$  is the turbulent heat flux, it is done by Eq. (5).

$$-\overline{\mathbf{u}_{j}t} = \alpha_{t} \frac{\partial \mathbf{T}}{\partial \mathbf{x}_{i}} \tag{5}$$

where,  $\alpha_t = \frac{\mu_t}{\alpha P_r}$  and  $P_r$  is Prandtl number=0.74.

The SST k- $\omega$  turbulence model [21] is used in this analysis. This model includes equations for turbulent kinetic energy k and the specific dissipation rate  $\omega$ . These have been expressed in Eqs. (6) and (7).

$$\frac{\partial (\rho V_{j} k)}{\partial x_{i}} = \frac{\partial}{\partial x_{i}} \left[ \Gamma_{k} \frac{\partial k}{\partial x_{i}} \right] + G_{k} - Y_{k}$$
 (6)

$$\frac{\partial (\rho V_{j}\omega)}{\partial x_{j}} = \frac{\partial}{\partial x_{j}} \left[ \Gamma_{\omega} \frac{\partial \omega}{\partial x_{j}} \right] + G_{\omega} - Y_{\omega} + D_{\omega}$$
 (7)

 $\Gamma_{k/\omega}$  denotes the effective diffusion coefficients,  $G_k/_\omega$  are the production rates,  $Y_{k/\omega}$  represents the dissipation rates of k and  $\omega$ , and  $D_\omega$  stands for the cross diffusion term.

The local Nusselt numbers is calculated according to the definitions presented in the Eq. (8), where q is the local heat flux density.  $T_j$  is the jet temperature and  $T_w$  is the wall temperature, it is considered constant in this work.  $\lambda$  is the thermal conductivity.

$$Nu = \frac{q}{(T_i - T_w)} \cdot \frac{D}{\lambda}$$
 (8)

The average Nusselt number is done by the Eq. (9) where Q is the heat flux integrated over the whole target surface plat with radius R.

$$\overline{Nu} = \frac{Q}{\pi R^2 (T_j - T_w)} \cdot \frac{D}{\lambda}$$
 (9)

The performance is evaluated as follows [22]:

$$PEC = \frac{Nu_{with tab} / Nu_{flat plate}}{(f_{with tab} / f_{flat plate})^{1/3}}$$
(10)

The skin frinction coefficient can be determined by the following formula [22]:

$$f = \frac{2D_h \Delta P}{V_i^2 \rho L} \tag{11}$$

where,  $\Delta P = P_{in} - P_{out}$ .

#### 2.3 Boundary conditions

The boundary conditions implanted in the computational domain as presented in Figure 1 are as follow:

- 1. Axis of symmetry: the variation of the dependent variables relative to the radius is zero  $(\frac{\partial V_x}{\partial r} = \frac{\partial k}{\partial r} = \frac{\partial \omega}{\partial r} = \frac{\partial T}{\partial r} = 0)$  and the radial velocity component  $V_r = 0$ .
- 2. Jet inlet: The jet velocity  $V_j$  is uniformly imposed and adjusted according to the specified Reynolds number (12). The turbulent intensity is set to I=4%, and the jet temperature is  $T_j$ =323 K.

$$Re = \frac{\rho V_j D_H}{\mu}$$
 (12)

- 3. Impingement plate and vortex generator: They are treated as a solid wall with no-slip conditions and Tw=277 K.
  - 4. Free boundaries: where atmospheric pressure is imposed

with ambient temperature T=298 K.

#### 2.4 Numerical method details

Ansys Fluent 14.5 was used to solve the governing equations through the Finite Volume Method. Velocity-pressure coupling was solved using SIMPLE. Second-order upwind discretized convective terms. Several convergence criteria of the numerical solution were tested (10<sup>-5</sup>, 10<sup>-7</sup> and 10<sup>-9</sup>), and gave similar results, hence 10<sup>-5</sup> were chosen to accelerate the calculation time.

The computational domain was meshed with uniform grid composed of square cells in majority to ensure good quality mesh. Various mesh sizes were tested, as outlined in Table 1, and it was determined that using 162,730 nodes (M2) provided accurate and computationally efficient results. Further mesh refinement yielded negligible improvements in results while increasing computational time and cost, as shown in Table 1.

Table 1. Effect of grid on average Nu

Grid	Number of Nodes	Nu
M 1	74490	47.11
M 2	162730	47.51
M 3	227863	47.52

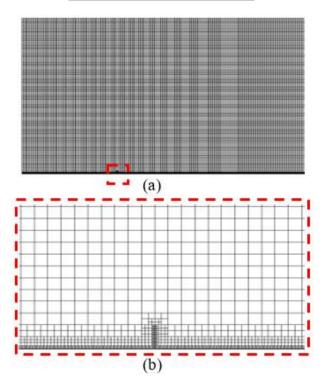


**Figure 2.** Mesh refinement details: a) mesh M2, b) mesh refinement around the tab

Figure 2 shows the considered generated grid M2 with a zoom around the generator vortex. Near the impact wall, the mesh was refined using the 'adapt' option several times in the Fluent solver, in order to always obtain a square shape of the mesh cells and avoid having stretched rectangular cells so to guaranty high mesh quality. The idea is also to obtain a sufficiently refined mesh near the impact wall to reach a value of  $y^+$  which represents the dimensionless space between the first node of the mesh and the wall, close to 1 ( $y^+ \le 1$ ). Additionally, Figure 3 displays the distribution of  $y^+$  from the wall along the target surface, using the grid M2, it can be

observed that  $y^+$  remains below one across the entire surface, allowing the application of the SST k- $\omega$  turbulence model.

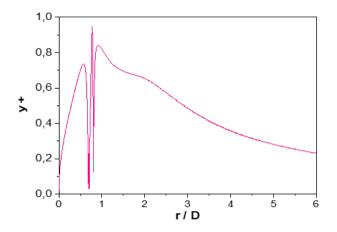
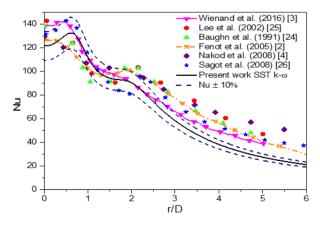


Figure 3. Radial distribution of y<sup>+</sup>

#### 3. RESULTS AND DISCUSSIONS

#### 3.1 Validation

Figure 4 illustrates the distribution of the Nu number along the target wall, with  $\pm 10\%$  deviation bands around the data. Using the SST k-ω turbulence model for a jet impinging on a flat surface with Re=23,000 and H/D=2. Simulation predictions show good agreement with both experimental results [2, 4, 23, 24] and numerical results [3, 25], particularly in the region of stagnation point and the region of the second peak at r/D=1.87 as reported by Fénot et al. [2]. However, a inconsistency with the experimental data is noted downstream of the flow for r/D > 3. This difference may be due to the constant temperature condition imposed to the wall in current simulations, whereas the reference data used a uniform wall heat flux as mentioned by Sagot et al. [25], Consequently, the numerical considerations in this study are validated. Consequently, the numerical considerations in this study are validated.

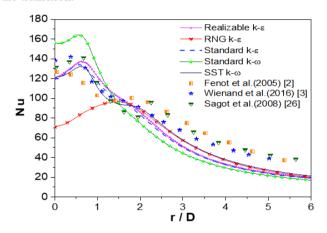


**Figure 4.** Comparison between the current result of Nu number with experimental data

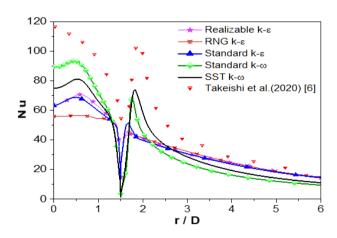
# 3.2 Turbulence modeling

Figure 5 presents a comparison of Nu distributions for various turbulence models with experimental data from the previous studies [2, 3, 25], to determine the most suitable

model through computational study. According to previous studies, jet impingement involves complex wall interactions. The results indicate that the SST k-ω turbulence model provides predictions closer to experimental data, particularly concerning the type and location of the secondary peak in the Nu. Nevertheless, some discrepancies were observed in other locations compared to experimental results, the secondary peak is linked to the transition to turbulent flow in wall iet regions as mentioned by Ashforth-Frost et al. [26]. Additionally, the standard k-ε and realizable k-ε models accurately predicted the Nusselt number at the stagnation point and surface Nusselt number distribution but failed to capture the secondary peak. Furthermore, the standard k-ω model overestimated the Nu\* value, while the RNG model showed a relatively large error in the local Nu calculation for a flat plate, making it unsuitable for the current study as it failed to capture the transition.



**Figure 5.** Local Nusselt numbers on flat plate estimated by various turbulence models compared to experimental data, Re=23000, H/D=2



**Figure 6.** Local Nusselt numbers on tabbed plate estimated by various turbulence models compared to experimental data, Re=10000, H/D=3

The analysis of jet impingement on a plate equipped with vortex generator presents challenging task due to the intricate flow dynamics involving stagnation, flow separation, and reattachment. To address this, Figure 6 presents a comparison of the Nu along the tabbed surface at H/D=3 and Re=10,000 with the experimental data from the study of Takeishi et al. [6], and tests different turbulence models to determine their effectiveness in handling this intricate case. The results show

that all turbulence models generally captured the peak, with noticeable discrepancies with the experimental results in position and magnitude. The SST k- $\omega$  model showed a dip and peak in the Nu in nearly the identical spot as observed by Takeishi et al. [6]. Despite some discrepancies, the overall trend in the calculated results aligns with the experimental findings. The peak in Nu is attributed to flow separation and reattachment induced by the tab, leading to recirculation zones before and after the tab that enhance heat transfer. Consequently, the following simulations will be carried out with SST k- $\omega$  turbulence model.

#### 3.3 Effect of presence of tab on heat transfer

Figure 7 demonstrates how the presence of a tab affects the distribution of the Nu in comparison to a flat plate for Re=23,000 and H/D=2, with the tab positioned at a radial distance L/D=0.7. The figure indicates a stagnation region with reduced velocities due to flow separation, leading to a dip in Nusselt number However, behind of the tab, there is a rapid increase in heat transfer attributed to the generation of vortices, which enhances turbulence and aids flow reattachment to the surface, thereby improving convective heat transfer. Moreover, a low-pressure zone forms behind the tab due to flow recirculation, as illustrated in Figures 8 and 9. The pressure contours and streamlines around the tab are depicted. The generation of vortices and flow separation near the tab increases turbulence kinetic energy, resulting in enhanced heat and turbulent momentum transfer as depicted in Figure 10. This heightened turbulence facilitates heat transfer behind the rib by disrupting the boundary layer, reducing its thickness, hence lowering thermal resistance and improving fluid-solid contact.

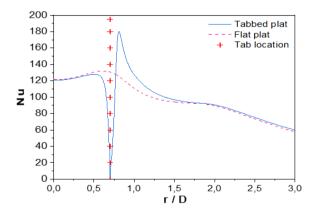


**Figure 7.** Nusselt number distribution at flat and tabbed plat, Re=23000, H/D=2, L/D=0.7,  $e/\delta=1$ 

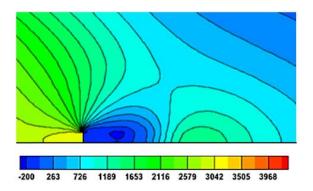


**Figure 8.** Contours of static pressure at L/D=0.7 and  $e/\delta=1$ 

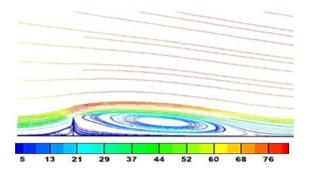


**Figure 9.** Streamlines around the tab at L/D=0.7 and  $e/\delta=1$ 

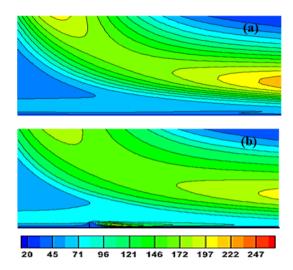


**Figure 10.** Contours of turbulent kinetic energy k at smooth surface (a) and tabbed surface (b)

# 3.4 Effect of Reynolds number

Figure 11 demonstrates the influence of Re number on the Nu distributions for a tabbed plate at H/D=2. Generally, an increase in Re improves heat transfer across all radial locations due to the increase in turbulent mixing, which enhances convective heat transfer coefficients. The increase is more significant near the tab due to the thinning of thermal and dynamic boundary layers, which reduces thermal resistance and improves heat transfer efficiency [27]. Additionally, the increase in the Re affects the Nu\* due to the increase in instantaneous velocities at the impingement point. In fact, as the Re number rises from 15,000 to 23,000, the Nu at the peak location increases by 38.3%, and by 30% at the stagnation point, highlighting the Re number significant impact on peak heat transfer compared to wall jet heat transfer.

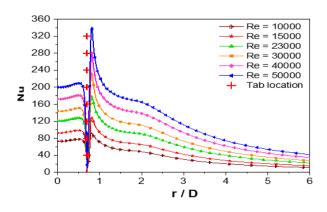
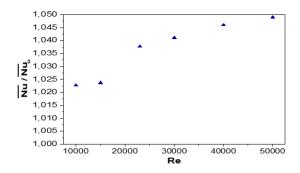


Figure 11. Nusselt profile for different Re number



**Figure 12.** The influence of Re on normalized average Nu number

In contrast, Figure 12 presents the impact of Re on the normalized  $\overline{Nu}$ . The figure shown that the highest heat transfer improvement was achieved at Re=50,000, This is due to the increased strength of turbulent vortex flows generated by the tab with increasing Re numbers.

## 3.5 Effect of nozzle-plate distance

Figure 13 depicts the Nu distributions for a tabbed plate at different H/D spacing with Re=23,000. Across all spacing, the greatest heat transfer is observed near the tab, indicating relatively intense turbulence in this region. Due to the presence of counter-rotating vortices with a gradual decrease in heat transfer towards the radial direction. Notably, at H/D=0.5 represents the maximum heat transfer in stagnation point, Perhaps due to the increase in momentum capacity and flow velocity upon impact. Additionally, another increase is observed at H/D=6. Suggesting that the development of turbulent flow structures while maintaining momentum the turbulence in the jet's shear layer is effectively penetrated at the center, increasing heat transfer rates, as mentioned by Gardon and Akfirat [28]. Figure 14 presents the influence of H/D on the normalized  $\overline{Nu}$ . The findings showed that an H/D=2 is the optimal spacing for enhancing heat transfer, this may be due to the appropriate development of the jet shear layer, which increases heat transfer rates.

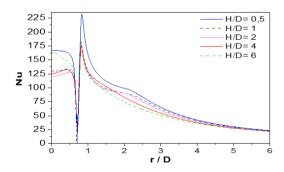
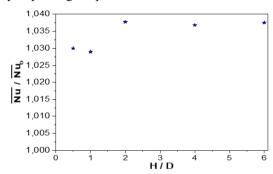


Figure 13. Nusselt profile for different H/D

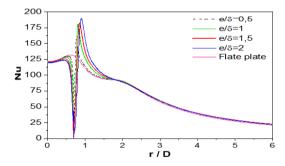
# 3.6 Effect of tab height

Figure 15 illustrates the impact of tab heights on the distribution of Nu numbers compared to a smooth surface when Re=23,000 and H/D=2. The tab is positioned at L/D=0.7. Serving as the reference point for normalized tab heights in this study. Based on previous studies [29] and as mentioned the thickness of the boundary layer of the wall jet  $\delta$  is assessed to be 0.02r. The figure demonstrates a noticeable peak in the Nu at the tab location, which increases with increasing tab

height, that is due to the formation of vortex structures, which become more effective with the increase in tab height. a lowpressure zone forms behind the tab and intensifies with increasing tab height, as depicted in Figure 16, because to formation of recirculation zones and increased turbulent mixing. Figure 17 illustrates the influence of tab height on the normalized  $\overline{Nu}$ . It is evident that the optimal value for enhancing heat transfer occurs when the tab height is adjusted to align with the  $\delta$ . These findings were confirmed by previous studies using DNS and LES calculations [17]. Additionally, improvements in the  $\overline{Nu}$  were compared with those reported by [7], who observed a 6% enhancement at a vortex generator position of 2, Takeishi et al. [6], who reported a 4.8% improvement at position 5, and Ortega-Casanova and Molina-Gonzalez [5], who found a 3.5% increase when using a single row of VG. This configuration helps maintain a thin and attached boundary layer, prevents flow separation, it also ensures an effective disruption of the boundary layer without causing excessive pressure drop or adverse effects on the flow, thereby improving the performance of heat transfer.



**Figure 14.** The influence of H/D on normalized average Nu number



**Figure 15.** Nusselt profile for different tab height  $e/\delta$ 

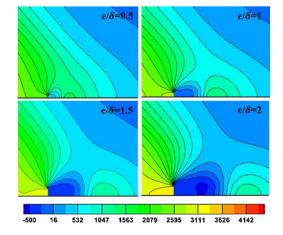


**Figure 16.** Contours of static pressure at L/D=0.7 for different tab heights  $e/\delta$ 

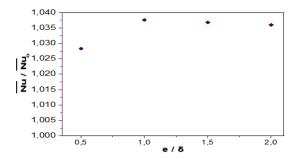


**Figure 17.** The influence of tab heights on normalized average Nu number

The Figure 18 illustrates the variation of the PEC for different tab height. The highest PEC value occurs at  $e/\delta=1$ , indicating the optimal value where thermal enhancement dominates over pressure drop. However, a slight decrease is observed with an increase in tab height, which may be due to energy and momentum losses caused by strong vortices that outweigh the benefits of heat transfer.

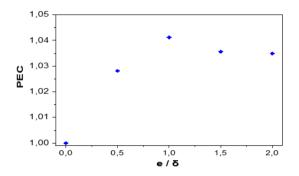


**Figure 18.** Variations of PEC in terms of tab heights  $e/\delta$ 

#### 3.7 Effect of tab location

Figure 19 illustrates the impact of tab locations on the Nu for Re=23,000 and H/D=2. Based on previous calculations, it was determined that the most effective tab height is equal to the boundary layer thickness. Therefore, all tab heights in this study are normalized relative to this value. The results show that the presence of the tab generates vortices, which enhances the mixing of fluid near the surface. This mixing disrupts and reduces the thickness of the boundary layer, resulting to a minimize in thermal resistance at the solid-fluid interface, thereby increasing the heat transfer coefficient. The peak of Nu decreases as the distance from the tab to the stagnation zone increases, this can be ascribed to the reduced flow velocity upon arrival, due to the exchange of momentum between the impinging jet and the wall [30]. we observe a very small peak at the position 1/D=0.25. This is due to the incomplete development of vortices. The highest peak in Nu occurs when the tab is near the stagnation zone at 0.7D, due to the formation of an ideal vortex leading to intense turbulent mixing.

Figure 20 presents the influence of tab location on the normalized  $\overline{Nu}$ . The figure shown that the highest heat transfer occurs at L/D=0.7, with a 3.8% increase. Furthermore, the Nu declines as the increase in L/D due to the decrease in flow velocity and the production of weaker vortex structures away from the stagnation zone, located about 1.2D above the target wall, as mentioned in the study of Martin [29].

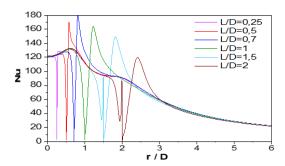
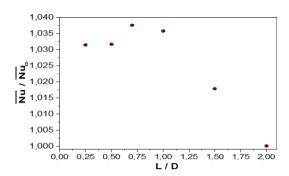


Figure 19. Nusselt profile for different tab location



**Figure 20.** The influence of tab locations on normalized average Nu number

On the other hand, Figure 21 illustrates the impact of the tab location on the normalized  $\mathrm{Nu}^*.$  The figure indicates that when the tab is positioned at radial distances less than 1 (L/D < 1),  $\mathrm{Nu}^*$  is always less than one compared to the flat plate. However, some improvement in  $\mathrm{Nu}^*$  is observed when the tab is positioned further from the impinging jet.

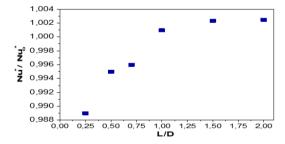


Figure 21. The influence of L/D on normalized Nu\* number

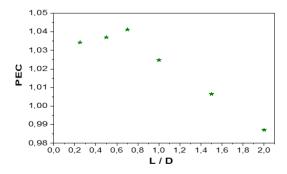


Figure 22. Variations of PEC in terms of tab locations L/D

The Figure 22 illustrates the effect of tab position on the variation of the PEC. The highest values of PEC occur when the tab is placed near the stagnation zone, especially at L/D=0.7, This may be due to the balance between turbulent

vortex intensity and momentum transfer, which enhances heat transfer efficiency relative to the penalties of pressure drop. With the increase in L/D, a decrease in the PEC is observed. This can be attributed to the reduction in turbulence intensity and energy dissipation, leading to lower effectiveness.

#### 3.8 Correlations

The correlations presented in this study prove to be valuable for predicting thermal performance and determining optimal geometric parameters in specific applications of jet impinging a flat plat equipped with symmetrical tab. Both average and stagnation local Nusselt number ( $\overline{Nu}$  and  $\mathrm{Nu}^*$ ) are notably influenced by the Re, jet-to-plate distance H/D, tab height-to-boundary layer thickness ratio e/ $\delta$ , and tab location-to-jet diameter ratio L/D. The correlations by least square method of all numerical results obtained for jet impingement on a tabbed surface at constant temperature are provided in Eqs. (13) and (14) as follows:

$$\overline{Nu} = 0.019 \text{ Re}^{0.78 \text{ H}} / D^{-0.07 \text{ L}} / D^{-0.015 \text{ e}} / \delta^{-0.012}$$
 (13)

For  $10,000 \le Re \le 50,000$ ,  $0.5 \le H/D \le 6$ ,  $0.25 \le L/D \le 2$  and  $0.5 \le e/\delta \le 2$ .

$$Nu^* = 0.377 \text{ Re}^{0.577} \text{ H/D}^{-0.016} \text{ L/D}^{-0.0006} \text{ e/\delta}^{0.0002}$$
 (14)

For  $10,000 \le Re \le 50,000$ ,  $1 \le H/D \le 4$ ,  $0.25 \le L/D \le 2$  and  $0.5 \le e/\delta \le 2$ .

When H/D=0.5 and 6 the influence of L/D and  $e/\delta$  is negligible on the Nu\*. It can be expressed as a function of only Re as shown in Eqs. (15) and (16).

$$Nu^* = 0.48 Re^{0.58} \text{ For } 10,000 \le \text{Re} \le 50,000, \text{ H/D} = 0.5$$
 (15)

$$Nu^* = 0.97 Re^{0.51} \text{ For } 10,000 \le \text{Re} \le 50,000, \text{ H/D} = 6$$
 (16)

Additionally, Figures 23 and 24 demonstrate a good agreement between predicted data from these correlations (13) and (14) and actual measurements the regression coefficients for these correlations are approximately 99% and 97%; respectively, indicating a high level of accuracy and acceptability.

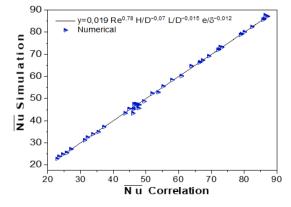
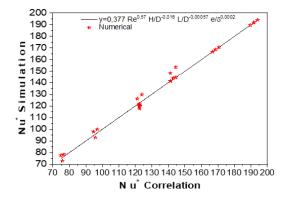


Figure 23. Comparison between the numerical results and correlation for  $\overline{Nu}$ 



**Figure 24.** Comparison between the numerical results and correlation for Nu\*

#### 4. CONCLUSIONS

A numerical investigation was conducted to study the impact of the height and location of a tab on the heat transfer between a turbulent jet impinging on a flat plate. The Re number ranged from 10,000 to 50,000, and distances from 0.5 to 6 between the jet and plate. Different positions of the vortex generator L/D were tested, ranging from 0.25 to 2, and various heights normalized by the boundary layer thickness  $e/\delta$  were examined, from 0.5 to 2. This study provided the distributions of heat transfer on the entire plate, with a particular focus on the vortex generator zone, aiming to evaluate the effectiveness of the tab in improving heat transfer. Overall, an increase in Re leads to enhanced heat transfer across all the radial locations due to the increased fluid velocity, which further enhances the momentum transfer and increases convective heat transfer coefficients. The maximum value of the Nu\* at H/D=0.5 and 6, which is attributed to the significant turbulence in these regions. The findings demonstrated that as the tab height increased, the Nu number downstream of the tab increased, attributed to the formation of a recirculation zone. which enhanced turbulent mixing and increase convective heat transfer. The highest increase in heat transfer was obtained when the tab height was adjusted to align with the  $\delta$ . when placing the tab near the stagnation region, a 3.8% enhance in heat transfer was achieved, which is attributed to the increased turbulence energy in that region. It's worth noting that the specific dimensions and optimal height of the tab may vary depending on the specific application, flow conditions, and desired heat transfer enhancement. In addition, a correlation was evolved for the  $\overline{Nu}$  and the Nu\*, based on the tab surface configuration investigated in this study.

### REFERENCES

- [1] Baughn, J.W., Shimizu, S. (1989). Heat transfer measurements from a surface with uniform heat flux and an impinging jet. Journal of Heat Transfer (Transactions of the ASME (American Society of Mechanical Engineers), Series C); (United States), 111(4): 6064124. https://doi.org/10.1115/1.3250776
- [2] Fénot, M., Vullierme, J.J., Dorignac, E. (2005). Local heat transfer due to several configurations of circular air jets impinging on a flat plate with and without semiconfinement. International Journal of Thermal Sciences,

- 44(7): 665-675. https://doi.org/10.1016/j.ijthermalsci.2004.12.002
- [3] Wienand, J., Riedelsheimer, A., Weigand, B. (2017). Numerical study of a turbulent impinging jet for different jet-to-plate distances using two-equation turbulence models. European Journal of Mechanics-B/Fluids, 61: 210-217.
  - https://doi.org/10.1016/j.euromechflu.2016.09.008
- [4] Nakod, P.M., Prabhu, S.V., Vedula, R.P. (2008). Heat transfer augmentation between impinging circular air jet and flat plate using finned surfaces and vortex generators. Experimental Thermal and Fluid Science, 32(5): 1168-1187.
  - https://doi.org/10.1016/j.expthermflusci.2008.01.009
- [5] Ortega-Casanova, J., Molina-Gonzalez, F. (2017). Axisymmetric numerical investigation of the heat transfer enhancement from a heated plate to an impinging turbulent axial jet via small vortex generators. International Journal of Heat and Mass Transfer, 106: 183-194.
  - https://doi.org/10.1016/j.ijheat mass transfer. 2016. 10.064
- [6] Takeishi, K.I., Krewinkel, R., Oda, Y., Ichikawa, Y. (2020). Heat transfer enhancement of impingement cooling by adopting circular-ribs or vortex generators in the wall jet region of a round impingement jet. International Journal of Turbomachinery, Propulsion and Power, 5(3): 17. https://doi.org/10.3390/ijtpp5030017
- [7] Alenezi, A.H., Almutairi, A., Alhajeri, H.M., Addali, A., Gamil, A.A. (2018). Flow structure and heat transfer of jet impingement on a rib-roughened flat plate. Energies, 11(6): 1550. https://doi.org/10.3390/en11061550
- [8] Tan, L., Zhang, J., Xu, H. (2014). Jet impingement on a rib-roughened wall inside semi-confined channel. International Journal of Thermal Sciences, 86: 210-218. http://doi.org/10.1016/j.ijthermalsci.2014.06.037
- [9] Kotb, A., Askar, H., Saad, H. (2023). On the impingement of heat transfer using swirled air jets. Frontiers in Mechanical Engineering, 9: 1120985. https://doi.org/10.3389/fmech.2023.1120985
- [10] Zeiny, E., Farhadi, M., Sedighi, K. (2017). Numerical investigation of the simultaneous influence of swirling flow and obstacles on plate in impinging jet. International Journal of Heat and Technology, 35(1): 59-66. https://doi.org/10.18280/ijht.350108
- [11] Gentry, M.C., Jacobi, A.M. (1997). Heat transfer enhancement by delta-wing vortex generators on a flat plate: Vortex interactions with the boundary layer. Experimental Thermal and Fluid Science, 14(3): 231-242. https://doi.org/10.1016/S0894-1777(96)00067-2
- [12] Du, X., Feng, L., Li, L., Yang, L., Yang, Y. (2014). Heat transfer enhancement of wavy finned flat tube by punched longitudinal vortex generators. International Journal of Heat and Mass Transfer, 75: 368-380. https://doi.org/10.1016/j.ijheatmasstransfer.2014.03.081
- [13] Ali, S., Dbouk, T., Wang, G., Wang, D., Drikakis, D. (2023). Advancing thermal performance through vortex generators morphing. Scientific Reports, 13(1): 368. https://doi.org/10.1038/s41598-022-25516-4
- [14] Bansode, V.H., Verma, M., Naik, C.K., Pandhare, A., Anjinappa, C., Prakash, C., Majdi, A. (2024). Air-side heat transfer enhancement using Vortex Generators on heat transfer surfaces-A comprehensive review. Journal of Heat and Mass Transfer Research, 11(2): 255-272. https://doi.org/10.22075/JHMTR.2024.33774.1549

- [15] Caliskan, S. (2014). Experimental investigation of heat transfer in a channel with new winglet-type vortex generators. International Journal of Heat and Mass Transfer, 78: 604-614. https://doi.org/10.1016/j.ijheatmasstransfer.2014.07.043
- [16] Tian, L.T., He, Y.L., Lei, Y.G., Tao, W.Q. (2009). Numerical study of fluid flow and heat transfer in a flat-plate channel with longitudinal vortex generators by applying field synergy principle analysis. International Communications in Heat and Mass Transfer, 36(2): 111-120. https://doi.org/10.1016/j.icheatmasstransfer.2008.10.01
  - https://doi.org/10.1016/j.icheatmasstransfer.2008.10.01
- [17] Oda, Y., Takeishi, K. (2014). Concurrent large-eddy simulation of wall-jet heat transfer enhanced by systematically-deformed turbulence promoter. In International Heat Transfer Conference 15, Kyoto, Japan, pp. 9217-9229. https://doi.org/10.1615/IHTC15.ttr.009516
- [18] Dutta, R., Srinivasan, B., Dewan, A. (2013). LES of a turbulent slot impinging jet to predict fluid flow and heat transfer. Numerical Heat Transfer, Part A: Applications, 64(10): 759-776. https://doi.org/10.1080/10407782.2013.798577
- [19] Dutta, R., Dewan, A., Srinivasan, B. (2016). Large eddy simulation of turbulent slot jet impingement heat transfer at small nozzle-to-plate spacing. Heat Transfer Engineering, 37(15): 1242-1251. https://doi.org/10.1080/01457632.2015.1119592
- [20] Shukla, A.K., Dewan, A. (2018). Heat transfer and flow characteristics of turbulent slot jet impingement on plane and ribbed surfaces. Thermophysics and Aeromechanics, 25: 717-734. https://doi.org/10.1134/S0869864318050086
- [21] Menter, F.R. (1994). Two-equation eddy-viscosity turbulence models for engineering applications. AIAA Journal, 32(8): 1598-1605. https://doi.org/10.2514/3.12149
- [22] Tekir, M., Taskesen, E., Gedik, E., Arslan, K., Aksu, B. (2022). Effect of constant magnetic field on Fe3O4-Cu/water hybrid nanofluid flow in a circular pipe. Heat and Mass Transfer, 58: 707-717. https://doi.org/10.1007/s00231-021-03125-7
- [23] Baughn, J.W., Hechanova, A.E., Yan, X. (1991). An experimental study of entrainment effects on the heat transfer from a flat surface to a heated circular impinging jet. Journal of Heat Transfer (Transactions of the ASME (American Society of Mechanical Engineers), Series C); (United States), 113(4): 1023-1025. https://doi:10.1115/1.2911197
- [24] Lee, D.H., Won, S.Y., Kim, Y.T., Chung, Y.S. (2002). Turbulent heat transfer from a flat surface to a swirling round impinging jet. International Journal of Heat and Mass Transfer, 45(1): 223-227. https://doi.org/10.1016/S0017-9310(01)00135-1
- [25] Sagot, B., Antonini, G., Christgen, A., Buron, F. (2008). Jet impingement heat transfer on a flat plate at a constant wall temperature. International Journal of Thermal Sciences, 47(12): 1610-1619. https://doi.org/10.1016/j.ijthermalsci.2007.10.020
- [26] Ashforth-Frost, S., Jambunathan, K., Whitney, C.F. (1997). Velocity and turbulence characteristics of a semiconfined orthogonally impinging slot jet. Experimental Thermal and Fluid Science, 14(1): 60-67.

- https://doi.org/10.1016/S0894-1777(96)00112-4
- [27] Benmouhoub, D., Mataoui, A. (2013). Turbulent heat transfer from a slot jet impinging on a flat plate. Journal of Heat Transfer, 135(10): 102201. https://doi.org/10.1115/1.4024554
- [28] Gardon, R., Akfirat, J.C. (1965). The role of turbulence in determining the heat-transfer characteristics of impinging jets. International Journal of Heat and Mass Transfer, 8(10): 1261-1272. https://doi.org/10.1016/0017-9310(65)90054-2
- [29] Martin, H. (1977). Heat and mass transfer between impinging gas jets and solid surfaces. Advances in Heat Transfer, 13: 1-60. https://doi.org/10.1016/S0065-2717(08)70221-1
- [30] Bode, F., Patrascu, C., Nastase, I. (2021). Heat and mass transfer enhancement strategies by impinging jets: A literature review. Thermal Science, 25(4 Part A): 2637-2652. https://doi.org/10.2298/TSCI200713227B

#### **NOMENCLATURE**

- D diameter of jet, m
- e tab height, m
- H nozzle-plate distance, m
- h local heat transfer coefficient. W, m<sup>-2</sup>. K<sup>-1</sup>
- k turbulent kinetic energy, m<sup>2</sup>. s<sup>-2</sup>

- L stagnation-tab distance, m
- Nu nusselt number
- Nu\* nusselt number at the stagnation point
- Nu<sub>0</sub> nusselt number on a flat plate
- Nu average Nusselt number on tabbed plate
- P Pressure, Pa
- R plate radius, m
- Re number of Revnolds
- S surface of the plate, m<sup>2</sup>
- T temperature, K
- V velocity, ms<sup>-1</sup>

#### **Greek symbols**

- α thermal diffusivity, m<sup>2</sup>. s<sup>-1</sup>
- $\lambda$  thermal conductivity, W. m<sup>-1</sup>. K<sup>-1</sup>
- δ boundary layer thickness, m
- μ dynamic viscosity, kg. m<sup>-1</sup>. s<sup>-1</sup>
- ρ density, kg. m<sup>-3</sup>
- $\omega$  specific dissipation rate, s<sup>-1</sup>

#### **Subscripts**

- j jet
- t turbulent
- w wall